Japanese Journal of Applied Physics **53**, 07KF03 (2014) **REGULAR PAPER**
http://dx.doi.org/10.7567/JJAP.53.07KF03

Correction of change in propagation time delay of pulse wave during flow-mediated dilation in ultrasonic measurement of arterial wall viscoelasticity

Mitsuki Sato[1], Hideyuki Hasegawa[1,2], and Hiroshi Kanai[1,2*]

[1]*Graduate School of Biomedical Engineering, Tohoku University, Sendai 980-8579, Japan*
[2]*Graduate School of Engineering, Tohoku University, Sendai 980-8579, Japan*
E-mail: kanai@ecei.tohoku.ac.jp

Received November 29, 2013; revised January 31, 2014; accepted March 14, 2014; published online June 5, 2014

It is considered that the endothelial dysfunction occurs in the initial step of atherosclerosis. Although assessments of the endothelial function and viscoelastic properties of the intima-media region are important for the diagnosis of early-stage atherosclerosis, regional viscoelasticity has not yet been measured in vivo. Our group has developed an ultrasonic method for measuring the transient change in viscoelasticity during flow-mediated dilation (FMD). However, in this method, the stress (blood pressure) and strain of the intima-media region of the radial artery are measured in different arms, and the change in pulse wave velocity (PWV) due to FMD has not yet been considered. In the present study, we measured blood pressure waveforms using two pressure sensors, which were placed along the same radial artery for the ultrasonic measurement, to obtain blood pressure waveforms and estimate the PWV between the two sensors. Using the measured PWV, the pulse wave propagation time from the pressure sensor to the position of the ultrasound probe was corrected, and viscoelasticity was estimated from the corrected stress–strain relationship. In the basic experiment, we applied the proposed method to a silicone tube phantom and evaluated the accuracy of the estimation of viscoelasticity by comparing the ultrasonic measurement to the results of the tensile test. In the in vivo measurements, the change in the propagation time delay of the pulse wave was also corrected using the two pressure sensors and the stress–strain relationship of the radial arterial wall was then obtained to estimate viscoelasticity. Furthermore, a decrease in elasticity owing to FMD after recirculation was clearly observed, and the unstable temporal variation in viscosity was significantly reduced. These results demonstrated the improvement in the accuracy of the measurement of viscoelasticity by the proposed method.

1. Introduction

Cardiovascular diseases have been cited as the main cause of death in Japan, and the primary cause of such diseases is atherosclerosis. The initial step in atherosclerosis is considered to be the endothelial dysfunction.[1)] Also, the homeostasis of a vessel wall is abrogated[2)] and the inflammation of the inner layer is induced by atherosclerosis. Consequently, it is important for an early preventive treatment of atherosclerosis to noninvasively assess the endothelial function.

Endothelial cells react to the shear stress caused by blood flow and produce nitric oxide (NO).[3)] NO is a vasodepressor material and stimulates the vessel wall to relax.[4)] This function is important for maintaining the homeostasis of the vascular system. The flow-mediated dilation (FMD) method is used for the conventional evaluation of the endothelial function.[5–7)] The FMD method evaluates the endothelial function by measuring the change in the inner diameter of the brachial artery after the release of avascularization. However, this method cannot directly evaluate the mechanical properties of the arterial wall.

For a more sensitive and detailed evaluation of the endothelial function and vessel wall mechanical property, a method of measuring the transient change in viscoelasticity during FMD was developed by our group.[8–12)] However, in this method, stress (blood pressure) and strain (change in intima-media thickness) are measured in the radial artery in different arms. Moreover, the change in pulse wave velocity (PWV),[13,14)] which is the velocity of the pressure wave caused by the contraction of the heart and propagating through the blood vessel, due to FMD has not been considered.[15)] To solve such a problem, in the present study, we developed a device for measuring stress and strain in the same arm. Furthermore, blood pressure waveforms were measured with two pressure sensors placed along the radial artery, and the PWV between the sensors was estimated. Using the estimated PWV, the change in the propagation time delay of the pulse wave owing to FMD was corrected to obtain better estimates of the viscoelastic constants of the radial arterial wall.

2. Materials and methods

2.1 Measurement of stress–strain relationship

In the present study, the radial artery, one of the muscular arteries, was measured to obtain the FMD reaction by applying avascularization using a cuff. It is necessary to measure the stress–strain relationship of the arterial wall in order to estimate viscoelasticity.

For the left radial artery, waveforms of blood pressure were measured using pressure sensors placed on the skin surface over the radial artery. The measured waveforms were calibrated by systolic and diastolic blood pressures measured with a sphygmomanometer in the right arm. These waveforms of blood pressure were used as the stress acting on the arterial wall.

To determine strain, the minute change in the thickness of the radial arterial wall during a cardiac cycle was measured using the *phased-tracking method*.[16)] This method can measure such minute displacement by calculating the phase shift due to the change in the propagation time of an ultrasonic pulse owing to the displacement of a target. To obtain the change in thickness, the velocities of arterial wall boundaries [lumen-intima boundary (LIB) and media-adventitia boundary (MAB)] were estimated. Either velocity was determined from the phase shift of echoes in two consecutive frames. The phase shift of echoes was obtained using a complex cross-correlation applied to demodulated RF signals. From the estimated phase shift $\Delta\hat{\theta}(t)$, the average velocity $\hat{v}(t)$ of the arterial wall at the pulse repetition interval T was obtained as

$$\hat{v}(t) = -\frac{c_0}{2\omega_0}\frac{\Delta\hat{\theta}(t)}{T}, \tag{1}$$

where ω_0 and c_0 are the center angular frequency of the

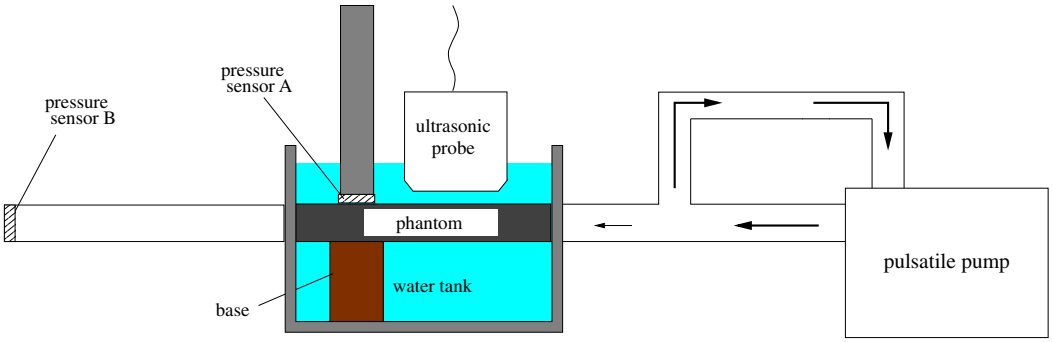

Fig. 1. (Color online) Illustration of basic experimental system.

ultrasonic pulse and the speed of sound, respectively. The change in thickness, $\Delta\hat{h}(t)$, between two different depths (LIB and MAB) was obtained from the difference between the displacements $\hat{x}_a$ and $\hat{x}_b$ at the LIB and MAB:

$$\Delta\hat{h}(t) = \hat{x}_a(t) - \hat{x}_b(t) = \int_0^t [\hat{v}_a(t) - \hat{v}_b(t)]\,dt, \quad (2)$$

where $\hat{v}_a$ and $\hat{v}_b$ are the velocities at the LIB and MAB, respectively.

The *phased-tracking method* has been used in various applications, e.g., measurements of the motion and deformation of the arterial and heart walls[17–19] for evaluating the viscoelastic properties and the myocardial function,[20–23] and measuring viscoelastic properties with acoustic radiation force.[24,25]

2.2 Correction of change in propagation time delay of pulse wave

PWV changes with some factors such as the elasticity and diameter of the artery, and the thickness of the arterial wall. Because it is difficult to measure ultrasonic RF signals and blood pressure waveforms in the same position, it is necessary to consider the propagation time delay of pulse waves. In the present study, blood pressure waveforms were measured with two pressure sensors placed along the radial artery to estimate the PWV between sensors. From the estimated PWV, the propagation time of the pulse wave from the pressure sensor to the position of the ultrasonic beam was estimated, and the temporal relationship between stress and strain was corrected.

The time delay between blood pressure waveforms, x_n and y_n, measured by the proximal and distal sensors was estimated using the cross-correlation function $r_{xy}(m)$

$$r_{xy}(m) = \frac{1}{N\sigma_x\sigma_y}\left(\sum_{n=0}^{N-1} x_n y_{n+m} - \bar{x}\bar{y}\right) \quad (3)$$

where (σ_x, σ_y) and $(\bar{x}, \bar{y})$ show the standard deviations and averages of the blood pressure waveforms, respectively. When the sampling frequency of the blood pressure waveforms is 10.3 kHz, the resolution in the estimation of time delay is approximately 0.1 ms.

2.3 Estimation of viscoelasticity from measured stress–strain relationship

Various models have been used to estimate the viscoelasticity of the blood vessel wall.[26–28] Let us assume that the viscoelastic property of the intima-media region of the arterial wall is modeled by the Voigt model.[29,30] The most simple viscoelastic model is the Voigt and Maxwell models. In the present study, the Voigt model was used because it is assumed that there is no permanent deformation in the arterial wall. We estimate elasticity and viscosity from the stress–strain relationship by modeling the stress $\hat{\tau}$ as

$$\hat{\tau}(t) = E_s \int \mathrm{LPF}[\dot{\gamma}(t)]\,dt + \eta\mathrm{LPF}[\dot{\gamma}(t)] + \tau_0, \quad (4)$$

where $\hat{\tau}(t)$ is the model of stress, and $\dot{\gamma}$, E_s, η, τ_0, and LPF$[\cdot]$ are the strain rate, static elasticity, viscosity coefficient, bias stress corresponding to diastolic pressure, and low-pass filter, respectively. The viscoelastic constants E_s and η and the diastolic blood pressure τ_0 (minimum blood pressure) are estimated using the least-squares method by minimizing the mean squared difference α between the measured stress $\tau(t)$ and the model $\hat{\tau}(t)$ defined by

$$\alpha = E_t[\tau(t) - \hat{\tau}(t)]^2, \quad (5)$$

where $E_t[\cdot]$ indicates the averaging operation with respect to time for a cardiac cycle.

3. Basic experiment using phantom

3.1 Experimental method using phantom

In the present study, the feasibility of the proposed method was validated using a cylindrical phantom made of silicone rubber containing graphite powder as scatterers (percent content: 3%). The wall thickness and inner diameter of the phantom were 1 and 8 mm, respectively. We used pulsatile flow to induce a pulsatile change in internal pressure.

The stress–strain relationship and viscoelasticity of the phantom were measured using the experimental setup illustrated in Fig. 1. As indicated in Sect. 2.2, blood pressure waveforms and PWV were measured with two pressure sensors placed along the radial artery in the in vivo experiment. Also, in the in vivo measurement, the radial artery was imaged in a short-axis view for the stable measurement of FMD, i.e., an ultrasonic beam could pass through the central axis of the artery even when the artery moved during the measurement due to avascularization. However, the length of the phantom was limited. Therefore, two pressure sensors (Kyowa PS-1KC) were placed as shown Fig. 1, and the phantom was imaged in the longitudinal-axis view to measure vibrations at two points along the phantom

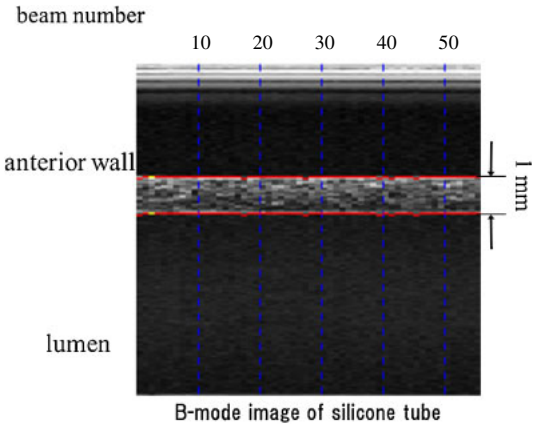

Fig. 2. (Color online) B-mode image of cylindrical phantom made of silicone rubber.

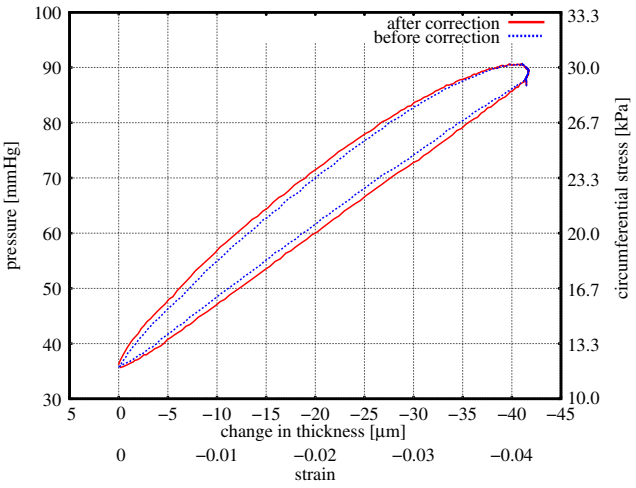

Fig. 3. (Color online) Stress–strain relationships with and without correction of propagation time delay of pulse wave measured in basic experiment.

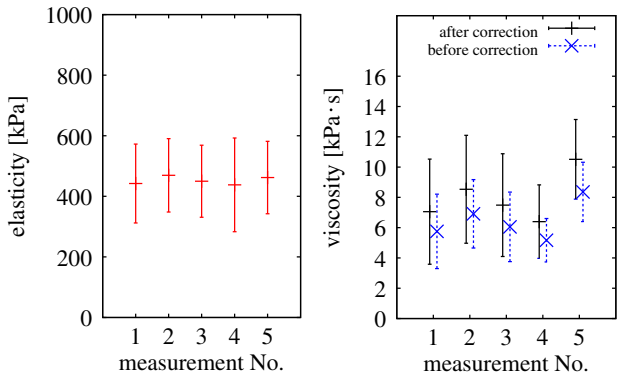

Fig. 4. (Color online) Elastic modulus and viscosity constant of phantom measured by US experiment.

for the estimation of pulse wave velocity. Blood pressure waveforms were measured using sensor A and calibrated using the highest and lowest values obtained by sensor B. The change in the wall thickness of the phantom was measured using a 22 MHz linear array ultrasonic probe (Diasus Dynamic Imaging). The sampling frequencies of the ultrasonic signal and blood pressure waveforms were 66.5 MHz and 10.3 kHz, respectively. Using the acquired ultrasonic signal, vibration velocities at the wall boundaries were obtained at two points (beams) along the phantom. By estimating the time delay between the waveforms of displacements measured at these two points, pulse wave velocity was obtained by dividing the distance between the two points (beams) by the estimated time delay. In this estimation, velocity waveforms were interpolated by a factor of 63 using reconstructive interpolation[31] because of the low sampling frequency (= frame rate) of velocity waveforms of 320 Hz. We corrected the propagation time delay of the pulse wave from pressure sensor A relative to the position of the ultrasound beam, and the viscoelasticity was estimated from the corrected stress–strain relationship.

3.2 Results of basic experiment

Figure 2 shows a B-mode image of the anterior wall of the phantom. The change in the thickness of the anterior wall caused by the change in internal pressure was measured. A pulsatile change in internal pressure was generated by a flow pump. In the basic experiment, the boundaries of the wall, which were tracked by the *phased-tracking method*, were initially determined automatically by thresholding the echo amplitude. The PWV was estimated using the cross-correlation function between the velocity waveforms in two ultrasonic beams. The mean PWV from five measurements was 6.95 m/s. The propagation time delay of the pulse wave from the ultrasonic beam to the pressure sensor was corrected using the estimated PWV.

Figure 3 shows the measured stress–strain relationship of the phantom wall with and without correction of the propagation time delay of the pulse wave.

To evaluate the accuracy of the proposed method, the viscoelastic constants of the phantom were also measured by a tensile test with a tensile tester (Autograph AG-X, Shimadzu, Japan). The elastic modulus and viscosity constant of the phantom were estimated to be 393 kPa and 42.4 kPa·s, respectively.

Figure 4 shows the mean and standard deviation of the elasticity and viscosity of the phantom, which were estimated from 20 beams by the proposed method. There was a very small change in elastic modulus. Therefore, values with and without correction were shown only for viscosity constants. In the ultrasonic measurement, the means of measured elasticity and viscosity were 452 kPa (before delay correction: 461 kPa) and 8.0 kPa·s (before delay correction: 6.4 kPa·s), respectively. The correction of the time delay mainly affects the estimation of viscosity. Elasticity was estimated with a mean error of about 50 kPa. The viscosity with correction became higher than that without correction and closer to the result obtained by the tensile test compared with the ultrasonic measurement with no correction. By correcting the propagation time delay of PWV, the time delay of strain from the pressure was increased, as well as the viscosity constant.

3.3 Discussion of basic experiment

In the basic experiment, the elasticity was estimated with a

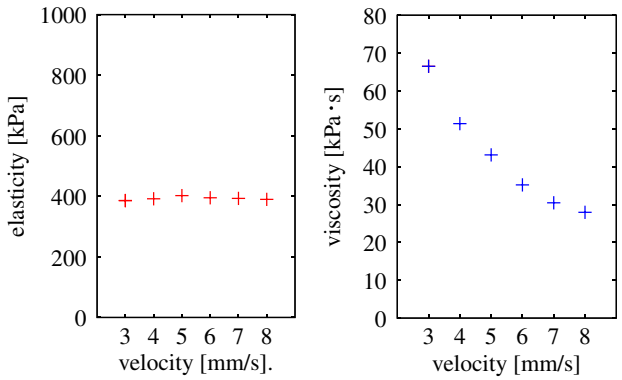

Fig. 5. (Color online) Elastic modulus and viscosity constant of phantom measured by tensile test.

small error of about 50 kPa. The viscosity with correction was closer to the result of the tensile test compared with the ultrasonic measurement with no correction. However, the absolute value of viscosity showed a large error of about 34 kPa·s. The reason for this error is considered to be the difference between the strain rates in the ultrasonic measurement and tensile test. There is a velocity dependence of the viscoelasticity of real materials. The maximum strain rate of the phantom was about 0.2 s^{-1} in the ultrasonic measurement. In Fig. 5, the viscoelasticity measured by the tensile tester was plotted as a function of the velocity of the jig of the tensile tester. The initial gage length was 55.2 mm and, thus, a jig velocity of about 11 mm/s matched with the strain rate of the ultrasonic measurement. However, only the velocity range shown in Fig. 5 was available in the tensile tester. Therefore, we considered the tendency of the relationship between strain rate (jig velocity) and viscosity constant. As can be seen in Fig. 5, the viscosity constant tends to decrease with jig velocity, i.e., the viscosity constants estimated by ultrasound and tensile test became closer when the strain rate in the tensile test was closer to that in the ultrasonic measurement. Therefore, it was considered that the error in the estimated viscosity constant was mainly caused by such a rate dependence.

4. In vivo experiment

4.1 In vivo experiment method

The left radial artery of a healthy male subject (23 years old) was measured in vivo. In this measurement, ultrasonic RF echoes (transmit: 22 MHz) were acquired at a sampling frequency of 66.5 MHz for 2 s and the frame rate was about 320 Hz. To evaluate FMD, the acquisitions were repeated every 20 s for 2 min at rest before avascularization and every about 20 s for 3 min after recirculation. We placed a cuff on the upper arm or forearm of the subject in order to perform avascularization to obtain the FMD reaction. Blood pressure waveforms in the left radial artery were measured with two pressure sensors. To support two pressure sensors and an ultrasonic probe, we have developed the device shown in Fig. 6. The waveforms measured by the distal sensor was used to obtain the stress–strain relationship. Blood pressure waveforms were acquired at a sampling frequency of 10.3 kHz, together with the acquisition of ultrasonic RF echoes.

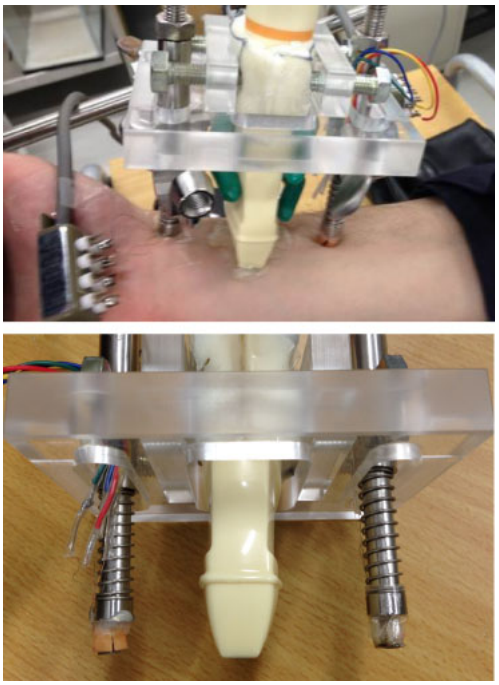

Fig. 6. (Color online) Device for in vivo measurement.

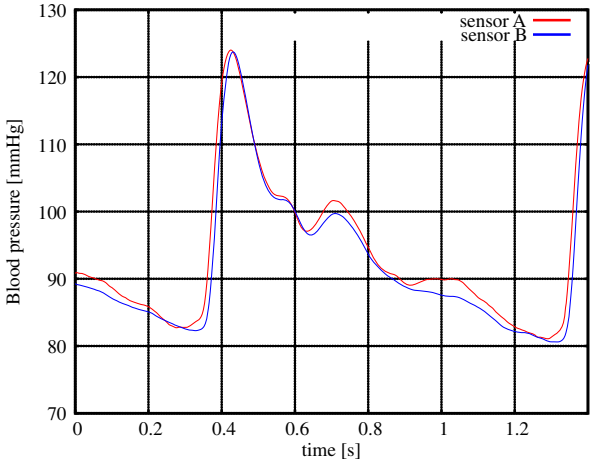

Fig. 7. (Color online) Blood pressure waveforms obtained by the proximal and distal sensors.

4.2 Results of in vivo experiment

The changes in arterial wall thickness and blood pressure were obtained for at least one cardiac cycle in each measurement to estimate the viscoelasticity of the radial arterial wall.

Blood pressure waveforms were measured at two points along the left radial artery using two pressure sensors. The distance between the two sensors was 74 mm. Figure 7 shows the measured blood pressure waveforms. We estimated the PWV by estimating the time delay using the cross-correlation function. Figure 8 shows the PWVs estimated pre- and post-avascularization. The black and blue lines in Fig. 8 show transient changes in the PWVs measured in the upper arm and forearm, respectively. Just after avascularization, the pulse wave velocity was very high, it then returns to pulse wave velocities similar to those at rest.

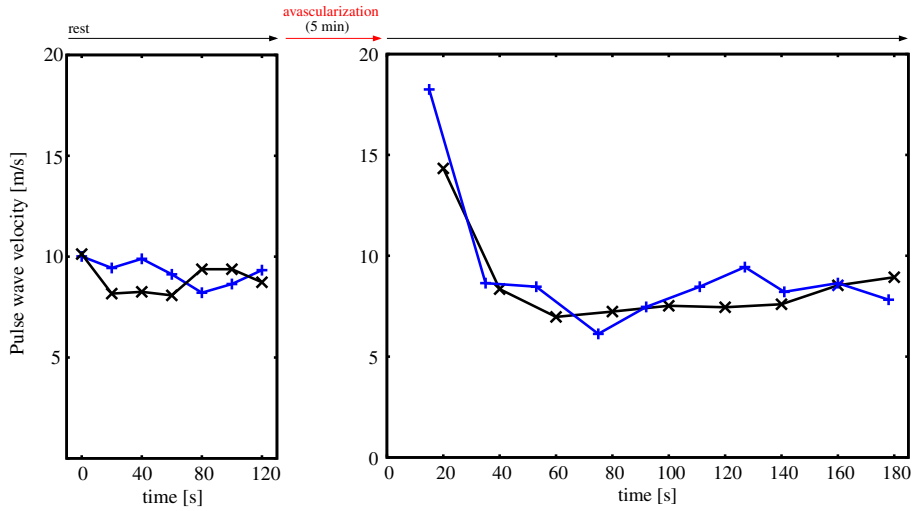

Fig. 8. (Color online) Transient changes in the pulse wave velocities estimated with avascularization in the upper arm (black) and forearm (blue).

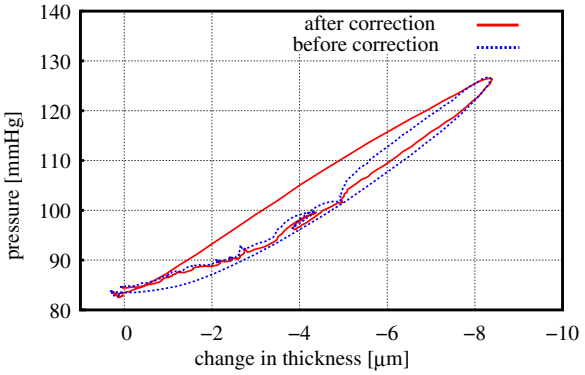

Fig. 9. (Color online) Measured stress–strain relationships with and without correction of propagation time delay of pulse wave.

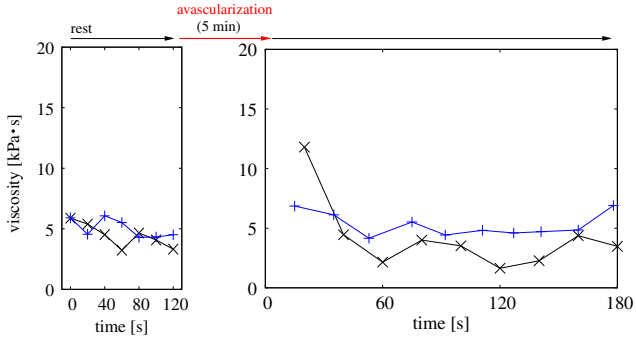

Fig. 11. (Color online) Transient changes in estimated viscosity constants. Avascularization was applied in the upper arm (black) and forearm (blue).

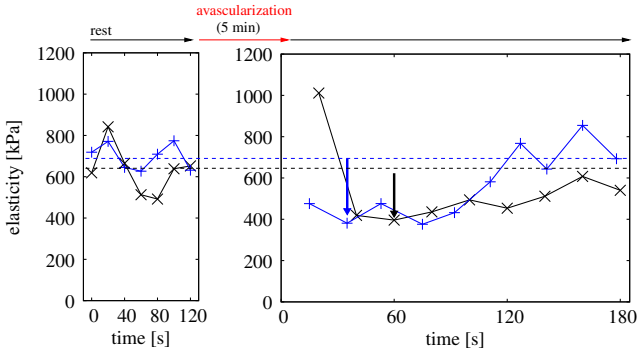

Fig. 10. (Color online) Transient changes in estimated static elasticity. Avascularization was applied in the upper arm (black) and forearm (blue).

Figure 9 shows the measured stress–strain relationships of the radial arterial wall with and without correction of the propagation time delay of the pulse wave. With correction, the directions of hysteresis loops were corrected from counterclockwise to clockwise.

Figure 10 shows the measured transient change in the static elasticity owing to FMD. The static elasticity shows an approximately 40% decrease after avascularization. Although the FMD reaction was found in both the upper arm and the forearm, the decrease in the elasticity by the avascularization measured in the upper arm occurred slower and longer than that measured in the forearm. In terms of the stability of the measurement, it is easier to induce avascularization in the upper arm than in the forearm because the upper arm is more distant from the positions of the ultrasonic probe and pressure sensors. Figure 11 shows the transient change in viscosity. The viscosity coefficients measured at rest are almost constant using the proposed correction of the propagation time delay of pulse waves. Just after recirculation, the viscosity coefficient became slightly lower than that at rest.

4.3 Discussion of in vivo experiment

In the in vivo measurement, the temporal decrease in the static elasticity E_s was observed after recirculation. This decrease in static elasticity is considered to be caused by the FMD reaction. The estimated viscosity was on the order of that measured in the carotid artery of dogs by in vitro experiments (5 kPa·s).[32] The viscosity coefficients measured at rest were almost constant, which showed the stable measurement achieved by the proposed correction. After recirculation, the viscosity coefficient became slightly lower than that at rest.

5. Conclusions

In the present study, we showed that the stress–strain relationship could be obtained correctly by considering the propagation time delay of pulse waves. We evaluated the accuracy of the estimation of viscoelasticity by the proposed method from a basic experiment using a cylindrical phantom made of silicone rubber. In the basic experiment, we estimated the viscoelasticity of the phantom by ultrasound and compared it with that measured by the tensile test. As a result, a better estimate of viscoelasticity could be obtained by the proposed method. In addition, in the in vivo measurement, we applied the proposed method to the measurement of the viscoelastic properties of the radial arterial wall by applying avascularization in the upper arm and forearm. The results show the potential of the proposed method for the thorough analysis of the transient change in viscoelasticity due to FMD.

1) R. Ross, New Engl. J. Med. **340**, 115 (1999).
2) P. O. Bonetti, L. O. Lerman, and A. Lerman, Arterioscler. Thromb. Vasc. Biol. **23**, 168 (2003).
3) H. Iwasaki, M. Shichiri, F. Marumo, and Y. Hirata, Endocrinology **142**, 564 (2001).
4) R. F. Furchgott, Circ. Res. **53**, 557 (1983).
5) M. C. Corretti, T. J. Anderson, E. J. Benjamin, D. Celermajer, F. Charbonneau, M. A. Creager, J. Deanfield, H. Drexler, M. Gerhard-Herman, D. Herrington, P. Vallance, J. Vita, and R. Vogel, J. Am. Coll. Cardiol. **39**, 257 (2002).
6) N. M. AbdelMaboud and H. H. Elsaid, Egypt. J. Radiat. Nucl. Med. **44**, 237 (2013).
7) T. Nakamura, Y. Kitta, M. Uematsu, W. Sugamata, M. Hirano, D. Fujioka, K. Sano, Y. Saito, K. Kawabata, J. Obata, and K. Kugiyama, Int. J. Cardiol. **167**, 555 (2013).
8) T. Kaneko, H. Hasegawa, and H. Kanai, Jpn. J. Appl. Phys. **46**, 4881 (2007).
9) K. Ikeshita, H. Hasegawa, and H. Kanai, Jpn. J. Appl. Phys. **47**, 4165 (2008).
10) K. Ikeshita, H. Hasegawa, and H. Kanai, Jpn. J. Appl. Phys. **48**, 07GJ10 (2009).
11) K. Ikeshita, H. Hasegawa, and H. Kanai, Jpn. J. Appl. Phys. **50**, 07HF08 (2011).
12) K. Ikeshita, H. Hasegawa, and H. Kanai, Jpn. J. Appl. Phys. **51**, 07GF14 (2012).
13) V. Govoni, M. L. Casagrande, F. Iqbal, and K. J. Cruickshank, Artery Res. **7**, 126 (2013).
14) C. Vlachopoulos, K. Aznaouridis, and C. Stefanadis, J. Am. Coll. Cardiol. **55**, 1318 (2010).
15) N. Onegbu, H. Kamran, B. Sharma, M. Bapat, S. Littman, N. Warrier, R. Patel, M. T. Khalid, L. Salciccioli, and J. M. Lazar, Atherosclerosis **220**, 151 (2012).
16) H. Kanai, M. Sato, Y. Koiwa, and N. Chubachi, IEEE Trans. Ultrason. Ferroelectr. Freq. Control **43**, 791 (1996).
17) K. Kitamura, H. Hasegawa, and H. Kanai, Jpn. J. Appl. Phys. **51**, 07GF08 (2012).
18) Y. Koiwa, H. Kanai, H. Hasegawa, Y. Saitoh, and K. Shirato, Ultrasound Med. Biol. **28**, 1395 (2002).
19) Y. Honjo, H. Hasegawa, and H. Kanai, Jpn. J. Appl. Phys. **51**, 07GF06 (2012).
20) M. Miyamoto, K. Kotani, K. Okada, A. Ando, H. Hasegawa, H. Kanai, S. Ishibashi, T. Yamada, and N. Taniguchi, J. Atheroscler. Thromb. **20**, 678 (2013).
21) K. Tsuzuki, H. Hasegawa, H. Kanai, M. Ichiki, and F. Tezuka, Jpn. J. Appl. Phys. **47**, 4180 (2008).
22) H. Shida, H. Hasegawa, and H. Kanai, Jpn. J. Appl. Phys. **51**, 07GF05 (2012).
23) H. Kanai and M. Tanaka, Jpn. J. Appl. Phys. **50**, 07HA01 (2011).
24) T. Sawada, H. Hasegawa, and H. Kanai, Jpn. J. Appl. Phys. **49**, 07HF10 (2010).
25) J. Yamaguchi, H. Hasegawa, and H. Kanai, J. Med. Ultrason. **39**, 279 (2012).
26) T. Khamdaeng, J. Luo, J. Vappou, P. Terdtoon, and E. E. Konofagou, Ultrasonics **52**, 402 (2012).
27) C. A. D. Leguy, E. M. H. Bosboom, H. Gelderblom, A. P. G. Hoeks, and F. N. van de Vosse, Med. Eng. Phys. **32**, 957 (2010).
28) J. J. R. Fojas and R. L. de Leon, APCBEE Procedia **7**, 86 (2013).
29) W. F. Walker, F. J. Fernandez, and L. A. Negron, Phys. Med. Biol. **45**, 1437 (2000).
30) K. R. Nightingale, M. L. Palmeri, R. W. Nightingale, and G. E. Trahey, J. Acoust. Soc. Am. **110**, 625 (2001).
31) Y. Céspedes, Y. Huang, J. Ophir, and S. Spratt, Ultrason. Imaging **17**, 142 (1995).
32) B. M. Learoyd and M. G. Taylor, Circ. Res. **18**, 278 (1966).